Highly efficient nonthermal ablation of bone under bulk water with a frequency-doubled Nd:YVO_4 picosecond laser

C. Tulea*, J. Caron, H. Wahab, N. Gehlich, M. Hoefer, D. Esser, B. Jungbluth, A. Lenenbach, R. Noll
Fraunhofer Institute of Laser Technology ILT, Steinbachstr. 15 52074 Aachen, Germany

ABSTRACT

Several laser systems in the infrared wavelength range, such as Nd:YAG, Er:YAG or CO_2 lasers are used for efficient ablation of bone tissue. Here the application of short pulses in coaction with a thin water film results in reduced thermal side effects. Nonetheless up to now there is no laser-process for bone cutting in a clinical environment due to lack of ablation efficiency. Investigations of laser ablation rates of bone tissue using a rinsing system and concerning bleedings have not been reported yet. In our study we investigated the ablation rates of bovine cortical bone tissue, placed 1.5 cm deep in water under laminar flow conditions, using a short pulsed (25 ps), frequency doubled (532 nm) Nd:YVO_4 laser with pulse energies of 1 mJ at 20 kHz repetition rate. The enhancement of the ablation rate due to debris removal by an additional water flow from a well-directed blast pipe as well as the negative effect of the admixture of bovine serum albumin to the water were examined. Optical Coherence Tomography (OCT) was used to measure the ablated volume. An experimental study of the depth dependence of the ablation rate confirms a simplified theoretical prediction regarding Beer-Lambert law, Fresnel reflection and a Gaussian beam profile. Conducting precise incisions with widths less than 1.5 mm the maximum ablation rate was found to be 0.2 mm^3/s. At depths lower than 100 µm, while the maximum depth was 3.5 mm.

Keywords: ablation rate, bulk water, bone tissue, plasma, blow-off model, OCT, ps-laser

1. INTRODUCTION

In the last decades many efforts have been made to replace mechanical tools in bone surgery by laser systems. The advantages of laser-induced ablation compared to mechanical drills and saws used in osteotomy are reduced mechanical stress, a more precise incision, the possibility to work without contact and the ability to superpose a diagnostic beam such as from an optical coherence tomograph [1-3]. The successful replacement of mechanical tools by lasers depends on the ablation efficiency and the avoidance of thermal damages induced by laserbeams, despite the fact that even conventional surgical saws induce temperature increase up to 100 °C and carbonization caused by friction, what leads to significantly reduced healing of the bone depending on the particular tool and its rotation speed [4, 5]. Therefore many investigations of laser-induced ablation were performed in the past. It was shown that pulsed laser systems in the microsecond to nanosecond regime using infrared wavelengths such as Er:YAG lasers, CO_2 lasers, Er:YSSG, Ho:YAG, FEL and Nd:YAG lasers are capable to perform incisions in hard tissue samples like dental enamel or bones under dry and wet conditions, while a water spray or a thin water film were used for cooling and to assist the ablation process [6-15]. For pulse lengths mentioned above a high linear absorption of the selected wavelength is necessary for an effective ablation process, therefore the laser systems that were used for bone cutting were chosen because of the absorption peaks of water and bone constituents in the infrared wavelength range [15].

The effects of wetting the tissue before and during the ablation process are twofold. Firstly a water spray as well as a water layer cause cooling to the tissue and lead to reduced thermal damage and less carbonization, while dry ablation generates severe carbonization, secondly the pressure of the water micro explosions leads to an enhanced ablation rate [10, 12]. Because tissue heating and thermal side effects still occur although water cooling is used, ultrashort (ps and fs) pulses for hard tissue ablation are investigated [6-19]. For ultrashort pulses, where the laser intensity in the focus exceeds 10^{11} W/cm^2, nonlinear absorption and multiphoton ionization lead to plasma mediated ablation [20]. According to Armstrong et al. this process is relatively independent of classic tissue properties [21], hence for ps- and fs-pulses also visible and ultraviolet wavelengths were used. Since for pulses shorter than the thermal relaxation times of tissue the penetration depth decreases beneath the thickness of the ablated layer, therefore ultrashort pulses are expected not to cause thermal

side effects on the surrounding tissue [20]. At the same time ps- and fs-pulses induce more precise and geometrically well defined incisions compared to longer pulses. Moreover the ablation threshold is reduced proportionally to the square root of the pulse duration [20]. However the ablation efficiency for ps-pulses was found to be higher than for fs-pulses [22]. Nonetheless thermal damage can still occur with ultrashort pulses applied due to heat accumulation depending on the repetition rate and pulse overlap. Visible thermal side effects and temperature increase were observed during ablation with ps pulses as well as with fs-pulses [17, 23]. Here visible and ultraviolet wavelengths seem to cause more thermal damage than infrared wavelengths [17]. For these reasons water cooling is used for ablation with ultrashort pulses in the same way as for pulses longer than some nanoseconds.

Yet the augmentation of the ablation efficiency of a thin water layer, that was applied on the tissue surface before the ablation process, or the usage of a water spray during the process are still not clear. Whereas some groups observed a slight reduction of the ablation rate under water spray conditions [17, 24], others report about increased ablation efficiency [12, 14]. Moreover the thickness of the water layer plays a role, actually a thick water layer reduces the rate of laser ablation [10]. Nevertheless an optimal thickness of the water layer cannot be specified. Even though the ablation of wet bones was investigated in many publications, there are no reports of hard tissue ablation where the probe is submerged several millimeters deep under bulk water. Though there is evidence suggesting, that the ablation under such liquid confinemend leads to higher plasma pressures directed towards the tissue surface and the formation of shock waves, that help to produce higher ablation rates compared to ablation in air [25]. Clear evidence was given by laser-induced breakdown spectroscopy of metals, where the ablated mass per pulse of a sample submerged 25 mm under water was more than four times higher compared to that of a probe in air [26]. Concerning, that short and ultrashort pulses may produce an optical breakdown in water and that the herewith produced plasma in water absorbs over 70 % of the laser energy before it can reach the target surface [27], particular attention has to be paid to the position of the beam waist to avoid the plasma shielding. Because plasma formation occurs in the focal volume for a fluence that equals the threshold fluence for optical breakdown and above the focus for higher fluences [25], the amount of ablated material is highest, when the target is positioned slightly above the geometric focal point [28].

Additionally to the effects of the presence of water during laser ablation, in this work it is shown that the movement of water i.e. a water flow has a further positive effect on tissue ablation. Particularly for incisions deeper than several hundreds of microns a water flow directed into the incision can help to remove the ablation debris. Absorption of the beam energy in the debris is one of the reasons for saturation of the cut depth with both increasing pulse number and pulse energy [12, 29]. Furthermore especially in surgery water flow is used to remove debris from the operating field. In this paper we describe the ablation of bones placed in a probe chamber 15 mm deep in under laminar and turbulent flow conditions. We investigated the effect of focus position and water flow on the cut depth and ablation efficiency. Because bleedings can occur during bone surgery, the effect of bleeding is studied by adding bovine serum albumin to the water. In literature it was shown that laser induced coagulation of blood constituents can cause reduced transmission [30], therefore we assessed the effect on the ablation rate of bovine serum albumin. Since a decrease of the ablation rate with the number of ablated layers was observed, the results are compared to theoretical predictions using a heuristic approach based on the blow-off model [25, 31].

In the literature no uniform definition of the ablation rate or ablation efficiency exists. The most common target parameters in the above cited articles are the depth per pulse given in µm, the ablated volume per pulse or mass per pulse in mm^3 or µg, the specific energy η in J/mm^3 respectively its reciprocal, the ablated volume per energy given in mm^3/J and sometimes the ablated mass per energy in µg/J. These parameters can only be converted one to another, when the scanning speed and the repetition rate of the laser and thus the pulse overlap and additionally the pulse energy is known. Hence sometimes it is not possible to compare different results of the ablation rate, especially when the depth per pulse is given without knowledge of the pulse overlap or the ablated volume per pulse. However, for surgical applications it is necessary to obtain a certain feed speed at given cut width and cut depth to compare the efficiency with that of mechanical drills and saws, because a given incision geometry in a certain tissue will usually take a certain amount of time to be cut by the surgeon. Therefore it is necessary to know the ablated volume per time. Consequently in this work, where the ablation rate is of interest, it will be denoted as the ablated volume per process time dV/dt given in mm^3/s, while the total process time to perform the incision is taken into account. Dividing this ablation rate by the product of the pulse energy E_p and the repetition rate f_R the ablation efficiency $1/\eta$ of one single pulse can be obtained easily.

2. SPECIMEN PREPARATION

Bovine femur bones were obtained from a local slaughter house. The periosteum and adherent fat was carefully removed with a scalpel, thereafter the cortical bone samples were cut into pieces of 2 x 3 x 0.5 cm^3 using a manual bonesaw. The surface of the bones was left unpolished as under real life conditions, although the energy coupling efficiency of a rough surface is reduced due to diffuse reflectance. The samples were maintained under room temperature and left to dry. Before ablation they were placed in the water filled probe-chamber described in the next section. The in vitro specimens cannot reflect the conditions in vivo, however Currey showed that rewetting dry bone samples restores the mechanical properties to values similar to those of living tissue [32]. Each ablation experiment was repeated for five different samples to obtain a mean value and a standard deviation.

3. EXPERIMENTAL SETUP

3.1 Laser ablation setup

A Nd:YVO_4 laser system was used to produce pulses with pulse durations of 25 ps at repetition rates of 10 kHz and 20 kHz. The laser light was amplified with a Slab amplifier [33] and frequency doubled to λ = 532 nm. Thereafter the maximum average output power was 14 W at 10 kHz and 20 W at 20 kHz. The power was measured before each ablation experiment with a thermal detector. The slightly elliptical beam had a beam quality of M^2_x = 1.7 and M^2_y = 1.3. The beam deflection was performed by a three-axis scanner system, consisting of a Galilean-telescope for focus shifting and a galvanometer scanner, then it was focused by a F-θ-lens with a focal length of f = 163 mm. In the focal plane the two beam radii were measured in air with a CCD-camera. These radii were used to calculate the effective fluence F_{eff} = 118 J/cm^2 for 20 kHz. From that fluence an effective beam radius in the focal plane assuming an ideal Gaussian beam can be calculated as $w_{0,eff}$ = 16.4 µm. The beam radius was also measured along the optical axis to estimate the Rayleigh length of the beam, which was z_R = 0.81 mm. Since the beam was focused into the water filled chamber, the refraction of the beam caustic at the water surface with refractive index n_w = 1.33 has to be taken into account. Hence the focus was shifted deeper into the water according to $l_{s,w} = n_w \cdot l_s$, where l_s is the height of the water layer above the original focal plane in air and $l_{s,w}$ is the depth of the focal plane from the water surface. Due to constancy of the beam parameter product the Rayleigh length is increased in water by the factor n_w^2 to $z_{R,water}$ = 1.43 mm.

To place each bone in the focal position before the ablation experiments, the axial position of the bone surface was varied at a pulse energy of 0.03 mJ, where visible plasma only occurs in the focal plane. By moving the bone surface in air along the optical axes with a micrometer translation stage until plasma became visible, the appropriate position of the surface with respect to the focal position in the water filled chamber could be calculated by the formula given above. By reason that the bone surface was not perfectly plane but slightly curved and curled, the focal position under water on the bone surface for a certain incision could only be estimated with an accuracy of 0.5 mm.

The focus of the beam was scanned in a meander pattern on the tissue surface to produce rectangular incisions. The scan speed v_{sc} in direction of the long incision edge (x-axis) was varied depending on the repetition rate of the laser from 1.4 m/s to 4 m/s, while the distance between neighboring lines in the perpendicular direction (y-axis) was 50 µm. The scan speed was chosen in such a manner that the pulse distance in the fast scan axis (x-axis) was three times the beam width in the focal plane. Nevertheless the appropriate choice of the scan speed combined with the laser repetition frequency ensured that for every new ablated layer the pulse positions were slightly changed. In consequence the pulse positions in the fast axis for the layer number k+1 coincided with the gaps in the layer k.

For every ablation experiment the total time to perform the incision was measured. The volume of the incision was measured afterwards with an OCT system with a total axial scan range of 9 mm, an axial resolution of 21,6 µm and a lateral resolution of 55 µm. The central wavelength of the OCT system was 1300 nm and the spectral bandwidth was 35 nm. In addition the incisions were analyzed with a visible and a scanning electron microscope to check whether thermal collateral tissue damage occurred and to check the geometrical homogeneity of the cut for the chosen pulse overlap.

3.2 Fluid system

In order to perform ablation experiments under bulk water with laminar and turbulent water flow, a probe chamber as illustrated in Figure was constructed and connected via silicon tubes to two different pump systems denoted as PS1 and PS2. At the entry of the laser beam an anti-reflection coated glass substrate made of fused silica was placed. The cham-

ber floor had a cavity of 3x2x1 cm^3 where the probe could be positioned with definite distance from the entrance window. The purpose of PS1 was primarily to flush the chamber with water, so that its full volume was filled with water up to the glass window, ensuring a constant and definite height of the water layer above the tissue surface. Its second purpose was to remove the ablated material from the interaction volume. The laminar flow within the water chamber was maintained by a rotary pump, which produced flow rates up to 6000 ml/min. The average flow velocity above the sample of the laminar water flow was 0.08 m/s.

PS2 delivered a liquid flow with pressures up to 22 bar to a nozzle with an inner diameter of d_n = 1 mm. This nozzle was inserted into the chamber through the silicon tubes of PS1. The bended tip of the nozzle was directed under a 45° angle at a distance of about 1 mm onto the bone surface. The direction of the fast scan axis (i.e. the axis of the long edge of the rectangular incision) was chosen to coincide with the direction of the water flow from both the laminar pump system and the high pressurized nozzle. At maximum system pressure of PS2 the flow rate in the nozzle was 900 ml/min and the average flow speed in the nozzle was calculated from that value to be 20 m/s. In conclusion the flow from PS2 was turbulent because of the high Reynolds number of R_e = 20000.

a) 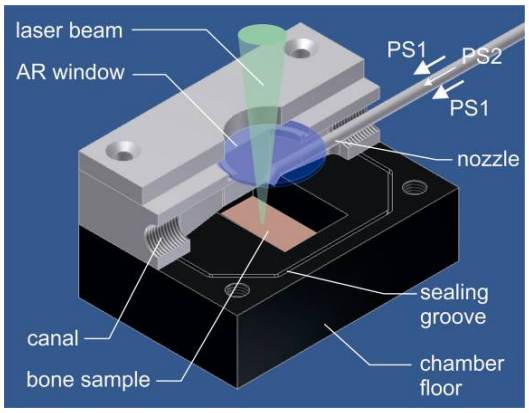

b) 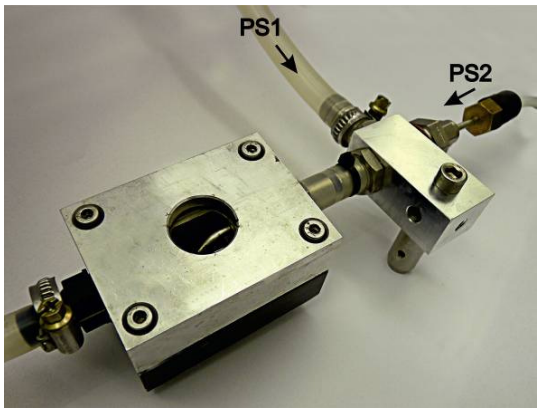

Figure 1. Water filled probe chamber with two fluid systems PS1 and PS2, a) three dimensional model and b) photograph of the chamber.

The force F_{hyd} of the water impact from the nozzle was calculated from the flow rate. Its maximum value was 0.3 N. This was confirmed by measurements with a laboratory scale under water, where the nozzle was directed onto the scale in a distance of 1 mm.

To simulate real life conditions, where bleedings can occur, bovine serum albumin (BSA) solution was used. In a first experiment 1 % BSA solution was added to PS1. The water was homogenously mixed with the solution and pumped through the water chamber with 4 l/min. The water from PS2 was left unchanged and applied with high pressure to the interaction zone. In a second experiment the effect of bleedings out of the incision was simulated by pumping full strength BSA solution with a flow rate of 20 ml/min through the nozzle directly into the incision, while the water from PS1was left clear.

4. RESULTS AND DISCUSSION

4.1 Effects of water and blood flow

Since the threshold of optical breakdown in water for 30 ps pulses at 532 nm wavelength is $3.8 \cdot 10^{11}$ W/cm^2 [34], the effect of the focus position with respect to the tissue surface was investigated, because the average pulse intensity in the focus at maximum pulse energy was one order of magnitude higher. Figure 2 shows the ablation rate with respect to the focal position, while the focus shift in the water chamber was considered according to section 3.1. This experiment was performed at 10 kHz with 1mJ pulse energy and a water filled probe chamber, while the second pump system PS2 was not in operation. To avoid effects of the aspect ratio, that will be described later, in this experiment 2 x 2 mm^2 squares were cut.

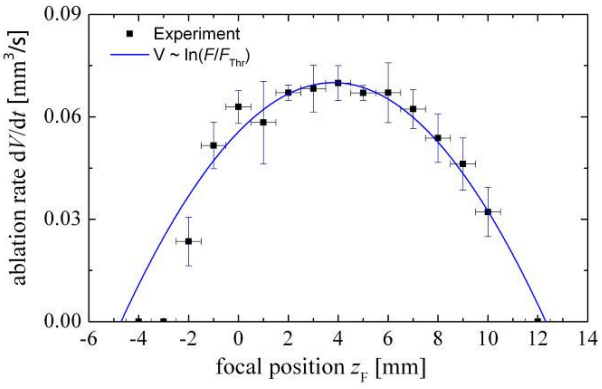

Figure 2. Ablation rate as a function of the axial position of the focus position with respect to the bone surface. The bone surface was at position $z_F = 0$ mm. Positive values indicate that the focus was below the surface. For negative values, the focus was in the water above the bone surface. The squares are the measured ablation rates with standard deviation according to variances from sample to sample and the solid line denotes a fit to the values according to the blow-off model.

Because of the divergent beam caustic and the constant scanning velocity of 2 m/s the pulse overlap was not constant in this experiment. The maximum ablation efficiency was achieved with the focus position about 4 mm inside the tissue. This result is consistent with the fact that plasma shielding due to an optical breakdown in water lowers the ablation efficiency. For even higher defocusing the ablation rate drops, because of the increasing beam waist on the surface, until the fluence falls below the threshold. With the measured beam radius at this position the threshold fluence was determined to be $F_{Thr} \approx 0.5$ J/cm^2. Within the standard deviation there the ablation rate is stable between $z_F = 2$ mm and $z_F = 6$ mm, this corresponds to changes in the focal position of more than twice the Rayleigh length. Nonetheless for the following experiments the focal position was set 4 mm below the tissue surface according to the maximum in the curve.

In Figure 3 the effect of the pump systems on the ablation rate was investigated for incisions, which were about 1 mm deep. Figure 3 a) and b) show the increase of the ablation rate, as a function of the water flow in PS1 and PS2. The system pressure of PS2 was increased from $p = 0$ bar to $p = 22$ bar. From the measured flow rate the flow speed and the hydrodynamic force were calculated. Here $p = 0$ bar equals the situation where no blast pipe at all i.e. only PS1 was used.

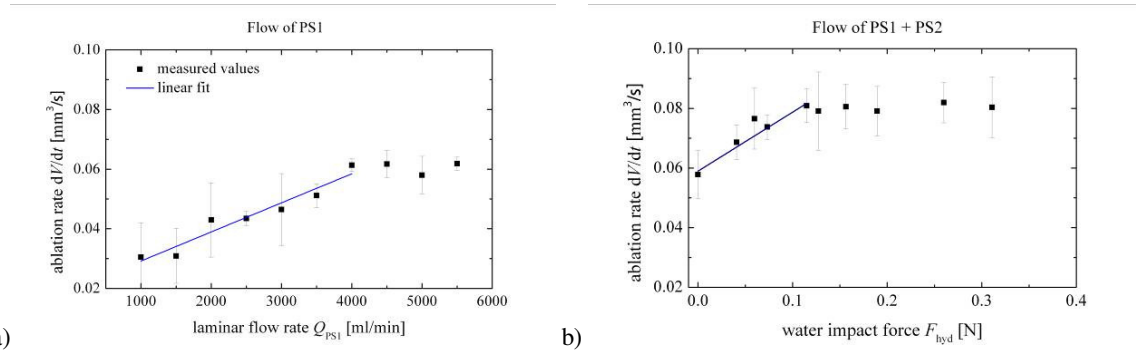

Figure 3. (a) Ablation rate for an increasing laminar flow rate in PS1. (b) Ablation rate for increasing system pressures in PS2 at $Q_{PS1} = 4000$ ml/min, leading to increasing impact force of the water. At $p = 22$ bar the maximum force of 0,31 N is reached. The forces 0.1 N, 0.2 N and 0.3 N correspond to flow rates in the nozzle of 570 ml/min, 731 ml/min and 937 ml/min.

Both the lateral laminar flow of water and the well directed turbulent water flow cause a similar effect on the ablation rate, while the combination of both increases the ablation rate by a factor of 2.7. A linear increase of the ablation rate is seen until it saturates. This saturation may occur, when no additional debris can be removed by the water flow. The linear increase with PS2 is seen up to a force of 0.11 N. This value corresponds to a system pressure of 6 bar, where a flow rate of 570 ml/min was measured. The average flow speed in the nozzle at this value was 11 m/s. For PS1 a minimum

flow rate of 1000 ml/min was necessary to keep the water height in the chamber constant, else air bubbles under the entrance window caused defocusing of the beam. With flow rates of 4000 ml/min from PS1 and 570 ml/min from PS2 the highest ablation rate was achieved. A further increase of the flow rates did not lead to higher ablation rates.

Because of the fact that the water flow from the nozzle was directed from one direction in a 45° angle into the incision, only the opposite side of the incision was affected by debris removal leading to increased depth and thus an increased ablation rate, as seen in Figure 4. In both cases the laminar and the turbulent flow came from left to right. Nonetheless only the water flow from the nozzle caused an asymmetrical cross sectional profile.

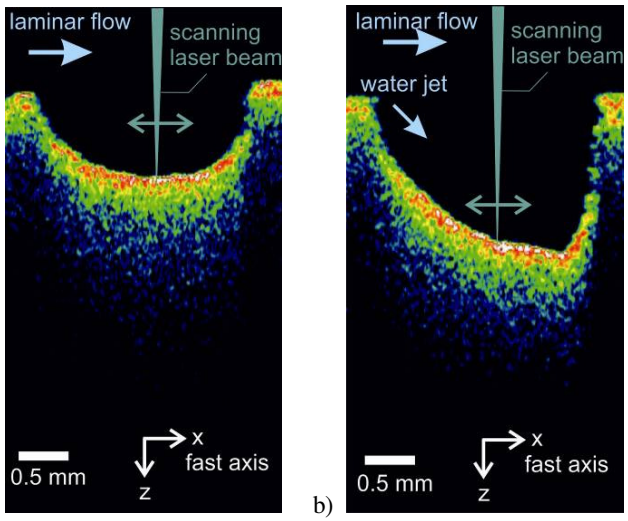

Figure 4. Color-coded OCT cross-sectional images along the fast axis of an incision (a) without and (b) with a well directed water flow from the nozzle.

In contrast to the augmented ablation rate by a purposeful water flow, additional BSA solution in the water was of negative effect, as shown in Figure 5.

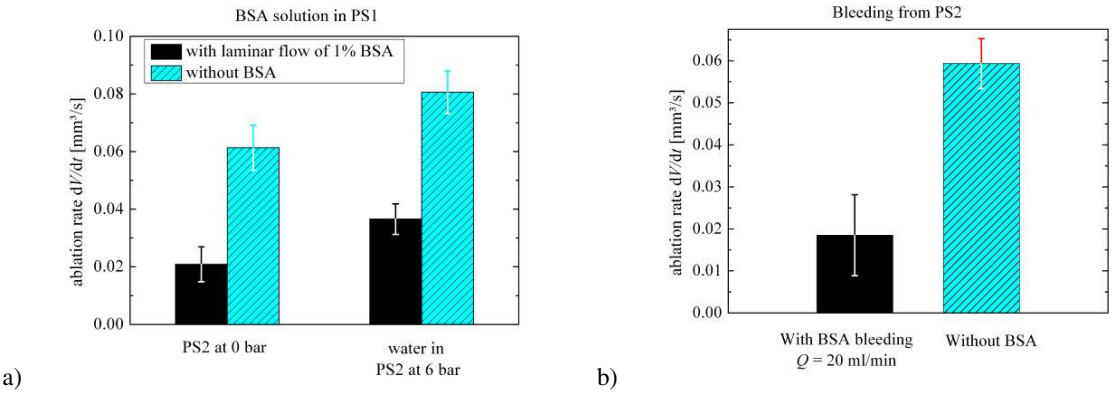

Figure 5. (a) Concentration of 40 g/l BSA solution depleted to 1 % in PS1. (b) Bleeding of pure 40 g/l BSA solution from PS2 with flow rate of 20 ml/min

First the 1 % of the 40 g/l BSA solution was mixed to PS1 with a flow rate of the mixture of 4000 ml/min. In the first experiment, where the PS2 was switched off, the ablation rate dropped down to 30 % of its initial value, when BSA solution was used. For the case that PS2 was operating at 6 bar with water, where the maximum ablation rate was expected, the decrease of the ablation rate with BSA solution was only 50 %. That means that the water flow from PS2 was effective in removing not only ablation debris but also blood by flushing the incision with pure water. In a second experiment,

PS1 provided pure water, while bleeding from the nozzle was simulated with native concentration of BSA at a flow rate of 20 ml/min. Here the ablation rate again decreased to 60 %. At a bleeding rate of 50 ml/min no ablation at all could be performed. Unfortunately the effect of PS2 at high pressure on removing the blood could not be investigated in the second experiment, since only one pump system of the type of PS2 was available.

4.2 Ablation depth

At higher aspect ratios the ablation rate decreased with the number of ablated layers, so the maximum achievable cut depth did not increase linearly with the number of ablated layers. To investigate this effect 4 mm long incisions with a width of 0.5 mm were cut at 20 kHz repetition rate with a scan velocity of 4 m/s. The maximum number of ablated layers was increased up to 20000. For 20000 layers the total duration to perform the incision was 310 s.

In the previous section we showed that the ablation rate depends on the focus position. Obviously the focus should be shifted with each ablated layer, when cutting incisions with depth in the order of the Rayleigh length of the laser beam. The depth dependence for a 0.5 mm broad incision on the focus shift per layer is shown in Figure 6. In this experiment PS2 was not used, to avoid any effects caused by the nozzle. The focus was shifted after each ablated layer into the surface. Here the initial focus position was set to be 4 mm inside the bone. The values for the focus shift per layer were estimated from the average cut depth per layer from the above experiments. The average value of the ablation depth per layer was 0.15 µm. Although this value decreases with the total depth, the focus shift was set to be constant for each layer. As seen in the figure, there is no dependence on the focus shift per layer up to a total depth of 2.4 mm. All curves correspond within their standard deviation, this is true even for the case where the focus was not shifted at all. For a focus shift per layer of 0.2 µm the total shift was 4 mm at a cut depth of 2.2 mm corresponding to 20000 ablated layers. For a focus shift per layer of 0.5 µm the total shift was 6.25 mm for 12500 layers at a cut depth of 2 mm. A total shift of 6.25 mm was already the limit of the Galilean telescope, therefore only 12500 layers were cut here. Compared to the Rayleigh length of $z_{R,water} = 1.4$ mm the total focus shift in the last experiment was more than four times higher than the focal length. Considering the initial focal position of $z_F = 4$ mm, the focus at the end of the ablation process was at $z_F = 10.25$ mm and thus 8 mm deeper than the tissue surface. Nevertheless the cut depth was within the standard deviation the same as for the experiment without focus shift, where the focus position at the end of the ablation process was only 2 mm under the tissue surface. These results together with the results in Figure 2 indicate that the focus position is not relevant, for cut depth marginally greater than the Rayleigh length as long as the focal plane lies inside the tissue.

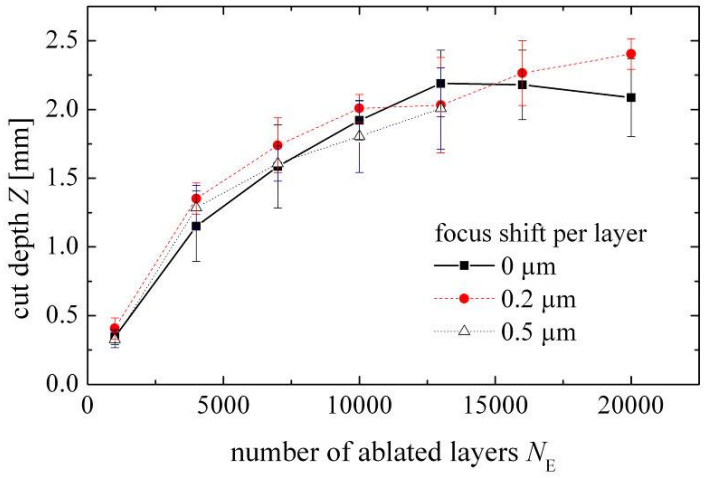

Figure 6. Maximum depth of the incision as a function of the number of ablated layers for three different focus shifts after each ablated layer. The solid lines are a guide to the eye. The total focus shift for each point is N_E times the focus shift per layer.

To compare the cross-sectional profile and the depth dependence with the blow-off model only the absorbed light has to be taken into account. The absorption is considered to follow the Beer-Lambert law and the portion of absorbed light is reduced by the Fresnel reflection with A = 1 – R, which is dependent on the polarization. Therefore the shape of the

incision as well as the ablation rate should depend on the polarization with respect to the plane of incidence. This was shown for homogeneous materials, for example for metals [35]. For this reason the ablation rate for both linear polarizations was measured in Figure 7. A half-wave plate was used to set the polarization. Within the standard deviation the polarization of the light had no influence on the ablation rate or the ablation depth.

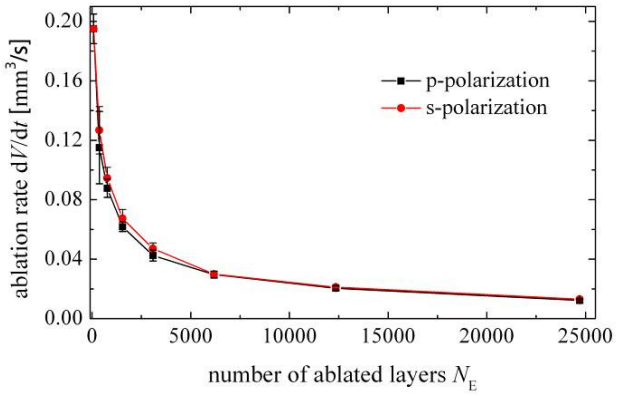

Figure 7. Ablation rate as a function of the number of ablated layers for s- and p-polarization.

In order to predict the total ablation depth a heuristic approach based on the blow-off model was used, which gives the depth dependence on the laser fluence. For a Gaussian beam profile this depth as a function of the fluence is logarithmic [25]. A space resolved calculation of the depth along the y-axis leads to the dashed line in Figure 8. Since the blow-off model does not consider absorption in the debris, both pump systems were used in the experiment, to remove the debris.

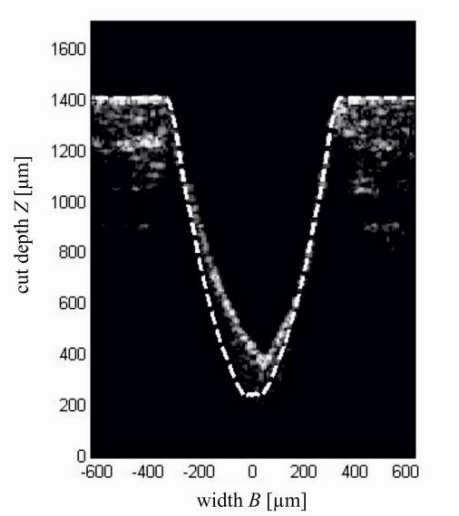

Figure 8. Comparison of the theoretically expected cross sectional shape with the experiment. Gray scale cross sectional OCT image along the slow axis of the beam profile for 770 layers compared to the simulated (dashed line) profile.

Figure 8 shows an OCT cross sectional image in comparison to the theoretically expected incision shape. The simulation describes the V-shaped beam profile very well. Still in the experiment the shape was asymmetric due to the water jet effect as can be seen in Figure 4. In the theory of course this was not concerned. Comparing the theoretically expected maximum ablation depth with the experiment, the calculated cut is about 10 % deeper than the experimental result.

4.3 Microscope images

No carbonization of the bone tissue was found after the ablation experiments. To investigate thermal side effects visual and scanning electron microscope images (SEM) were taken. These are shown in Figure 9. In the visual microscope images no evidence of thermal damage or any side effects to surrounding tissue was found. The SEM images however show structures at the crater edge (Figure 9d), which could originate from molten minerals. The side effect on the surrounding tissue is of the order of 10 µm. No collateral damage of the surrounding tissue for distances grater then 20 µm to the crater wall were observed.

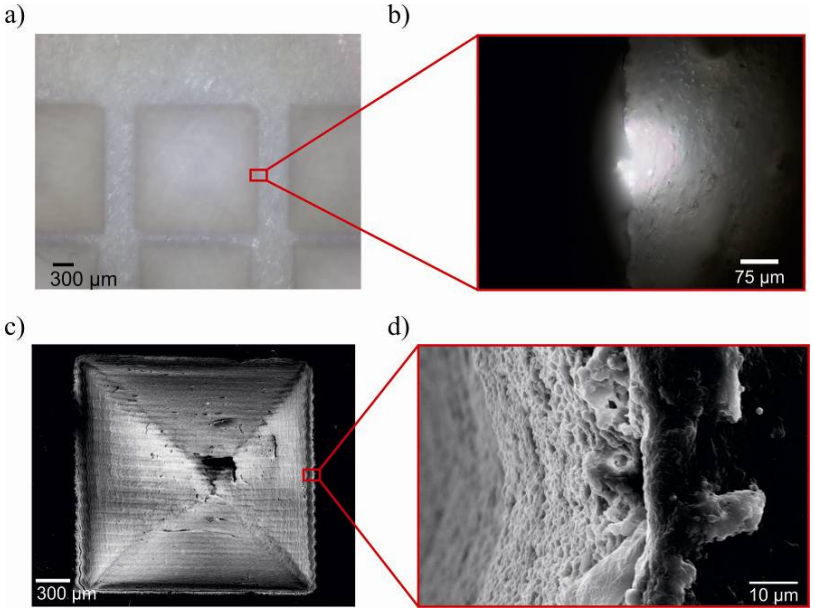

Figure 9. a) Visual microscope image of a 2 x 2 mm^2 incision in cortical bone at a magnification of 25 and b) 100. c) and d) REM images of the incision.

5. CONCLUSIONS

We have investigated the ablation of bovine cortical bone tissue samples under bulk water with a picosecond laser at visible wavelength of 532 nm that produced 1 mJ pulse energy at repetition rates of 10 kHz and 20 kHz. Using purposeful laminar and turbulent water flows, the ablation rate could be increased linearly until the debris was removed from the incision. The maximum ablation rate for shallow cuts of 125 µm depth was 0.2 mm^3/s with no evidence of thermal damage. For incisions deeper than 1 mm the averaged ablation rate over the total process time was 0.08 mm^3/s. The admixture of bovine serum albumin to the water environment lowered the ablation rate to 30 %. Due to the Gaussian beam profile and the angle-dependent reflection at the tissue surface the cross sections of the ablated incisions were V-shaped, which led to a limitation of the maximum cut depth. The maximum cut depth for 0.5 mm broad cuts was 2.4 mm.

REFERENCES

[1] Zahn, H., Jungnickel, V., Ertl, Th., Schmid, S., Müller, G., "Bone Surgery with Er:YAG Laser," Lasermedizin 13, 31-36, (1997).

[2] Winand, O., Morgenroth, K., "Experimentelle Osteotomien mit dem Er:YAG-Laser im Vergleich zu konventionellen Techniken," Laser Journal 2, 10-14, (2003).

[3] Targowski, P., Ostrowski, R., Marczak, J., Syswestrzak, M., Kawiatkowska, E. A., "Picosecond laser ablation system with process control by Optical Coherence Tomography," Proc. SPIE 7391, 7391-15, (2009)

[4] Hänisch, C. v., [Osteogenese nach Laserosteotomie mit einem CO_2-Laser im Vergleich zur Osteotomie mit konventioneller Sägetechnik – eine Tierexperimentelle Studie], Dissertation LMU Munich, Munich 39-82 (2004).
[5] Fuchsberger, A., "Untersuchung der spanenden Bearbeitung von Knochen," Springer, Berlin 120-124 (1986)
[6] Hibst, R., Keller, U., "Experimental Studies of the Application of the Er:YAG Laser on Dental Hard Substances: I. Measurement of the Ablation Rate," Lasers Surg. Med. 9, 338-344, (1989).
[7] Li, Z., Code, J. E., van de Merwe, W. P., "Er:YAG Laser Ablation of Enamel and Dentin of Human Teeth: Determination of Ablation Rates at Various Fluences and Pulse Repetition Rates," Lasers Surg. Med. 12, 625-630, (1992).
[8] Visuri, S. R., Walsh, J. T., Widgor, H. A., "Erbium Laser Ablation of Dental Tissue," Lasers Surg. Med. 18, 294-300, (1996)
[9] Rupprecht, S., Tangermann, K., Kessler, P., Neukam, F. W., Wiltfang, J., "Er:YAG laser osteotomy directed by sensor controlled systems," J. Cranio-Maxillofac.. Surg. 31, 337-342, (2003).
[10] Fried, D., Ashouri, N., Breunig, T., Shori, R., "Mechanism of Water Augmentation During IR Laser Ablation of Dental Enamel," Lasers Surg. Med. 31, 186-193, (2002).
[11] Assa, S., Meyer, S., "Ablation of Dental Hard Tissues with a Microsecond Pulsed Dioxide Laser Operating at 9.3-µm with an Integrated Scanner," Proc. SPIE 6843, 684308-1, (2008).
[12] Ivanenko, M. M., Hering, P., "Wet bone ablation with mechanically Q-switched high-repetition-rate CO_2 laser," Appl. Phys. B 67, 395-397, (1998).
[13] Stanislawki, M., Meister, J., Mitra, T., Ivanenko, M. M., Zanger, K., Hering, P., "Hard tissue ablation with a free running Er:YAG and a Q-switched CO_2 laser: a comparative study," Appl. Phys. B 72, 115-120, (2001).
[14] Kang, H. W., Lee, H. Chen, S., Welch, A. J., "Enhancement of Bovine Bone Ablation Assisted by a Transparent Liquid Layer on a Target Surface," IEEE J. Quantum Elect. 42, 633-642, (2006).
[15] Youn, J., Sweet, P., Peavy, G. M., "A Comparison of Mass Removal, Thermal Injury and Crater Morphology of Cortical bone Ablation Using Wavelengths 2.79, 2.9, 6.1 and 6.45 µm," Lasers Surg. Med. 39, 332-340, (2007).
[16] McCaughey, R. G., Sun, H., Rothholtz, V. S., Juhasz, T., Wong, B. J. F., "Femtosecond laser ablation of the stapes," J. Biomed. Opt. 14, 024040-1, (2009).
[17] Bello-Silva, M. S., Wehner, M., de Paula Eduardo, C., Lampert, F., Poprawe, R., Hermans, M., Esteves-Oliveira, M., "Precise ablation of dental hard tissues with ultra-short pulsed lasers. Preliminary exploratory investigation on adequate laser parameters," Lasers Med. Sci., (2012).
[18] Girard, B., Yu, D., Armstrong, M. R., Wilson, B. C., Clokie, C. M. L., Dwane Miller, R. J., "Effects of Femtosecond Laser Irradiation on Osseous Tissues," Laser Surg. Med. 39, 273-285, (2007).
[19] Emigh, B., An. R., Hsu, E. M., Crawford, T. H. R., Haugen, H. K., Wohl, G. R., Hayward, J. E., Fang, Q., "Porcine cortical bone ablation by ultrashort pulsed laser irradiation," J. Biomed. Opt. 17, 02100-1, (2012).
[20] Niemz, M. H., [Laser-Tissue Interactions], Springer, Heidelberg, 58-150, (2007).
[21] Armstrong, W. B., Neev, J. A., Da Silva, L. B., Rubenchik, A. M., Stuart, B. C., "Ultrashort Pulse Laser Ossicular Ablation and Stapedotomy in Cadaveric Bone," Lasers Surg. Med. 30, 216-220, (2002).
[22] Kim, B. M., Feit, M. D., Rubenchik A. M., Joslin, E. J., Celliers, P. M., Eichler, J., Da Silva L. B., "Influence of pulse duration on ultrahort laser pulse ablation of biological tissues," J. Biomed. Opt. 6, 332-338, (2001).
[23] Neev, J., Da Silva, L. B., Feit, M. D., Perry, M. D., Rubenchik, A. M., Stuart, B. C., "Ultrashort Pulse Lasers for Hard Tissue Ablation," IEEE Quantum. Elect. 2, 790-800, (1996).
[24] Kang, H. W., Oh, J., Welch, A. J., "Investigations on laser hard tissue ablation under various environments," Phys. Med. Biol. 53, 3381-3390, (2008).
[25] Vogel, A., Venugopalan, V., "Mechanisms of Pulsed Laser Ablation of Biological Tissues," Chem. Rev. 103, 577-644, (2003).
[26] Pichahchy, A. E., Cremers, D. A., Ferris, M. J., "Elemental analysis of metals under water using laser-induced breakdown spectroscopy," Spectr. Acta B 52, 25-39, (1997).
[27] Vogel, A., Noack, J., Nahen, K., Theisen, D., Busch, S., Parlitz, U., Hammer, D. X., Noojin, G. D., Rockwell, B. A., "Energy balance of optical breakdown in water at nanosecond to femtosecond time scales," Appl. Phys. B 68, 271-280, (1999).
[28] Sylvestre, J.-P., kabashin, A. V., Sacher, E., Meunier, M., "Femtosecond laser ablation of gold in water: influence of the laser-produced plasma on the nanoparticle size distribution," Appl. Phys. A 80, 753-758, (2005).
[29] Mitra, Th., [Ablation biologischen Hartgewebes mit gepulsten IR-Lasern], Dissertation HHU Düsseldorf, Düsseldorf, (2002).

[30] Pfefer, T. J., Choi, B., Vargas, G., McNally, K. M., Welch, A. J., "Pulsed Laser-Induced Thermal Damage in Whole Blood," J. Biomed. Eng. 122, 196-202, (2000).
[31] Srinivasan, R., "Ablation of Polymers and Biological Tissue by Ultraviolet Lasers," Science 234, 559-565, (1986).
[32] Currey, J. D., "The effect of porosity and mineral content on the Young's Modulus of elasticity of compact bone," J. Biomech. 21, 131-139, (1988).
[33] Höfer, M., Traub, M., Kleindienst, R., Sipma, H., Hoffmann, H.-D., Wessels, P., Burdack, P., "Multi ten wat, ultra-stable and tuneable Innoslab based single frequency MOPA," Proc. of SPIE 6451, 64510S1-6, (2007).
[34] Noack, J., Vogel, A., "Laser-Induced Plasma Formation in Water at Nanosecond to Femtosecond Time Scales: Calculation of Thresholds, Absorption Coefficients, and Energy Density," IEEE Quant. Elec. 35, 1156-1167, (1999).
[35] Venkatakrishnan, K., Tan, B., Stanley, P., Sivakumar, N. R., "The effect of polarization on ultrashort pulsed laser ablation oft thin metal films," J. of Appl. Phys. 92, 1604-1607, (2002).